THE BLACK SILICON METHOD IV: THE FABRICATION OF THREE-DIMENSIONAL STRUCTURES IN SILICON WITH HIGH ASPECT RATIOS FOR SCANNING PROBE MICROSCOPY AND OTHER APPLICATIONS

Henri Jansen, Meint de Boer, Bert Otter, and Miko Elwenspoek

MESA Research Institute, University of Twente, P.O. Box 217, 7500 AE Enschede, The Netherlands

Phone: X-31-53-894373; Secr: X-31-53-892751; Fax: X31-53-309547

ABSTRACT

The recently developed black silicon method (BSM) is presented as a powerful tool in finding recipes for the fabrication of MEMS building blocks such as xy-stages, scanning probe tips, inkjet filters, multi-electrodes for neuro-electronic interfaces, and mouldings for direct patterning into polymers. The fabrication of these blocks in silicon with high aspect ratios and smooth surface textures will be described and discussed by using the BSM and standard reactive ion etching (RIE).

1. INTRODUCTION

Dry etching technology is indispensable for fabricating three-dimensional building blocks for MEMS applications. The fabrication technique of these blocks demand etching processes with high etch rate and -selectivity, both for bulk- and surface micromachining. For the exact definition of the structures with high aspect ratios it is necessary that the anisotropy and surface texture can be well controlled.

We have recently demonstrated that trenches (up to 200μm) with high aspect ratios (up to 10) in silicon are etched at high etch rates (up to 5μm/min) and low ion energies (15-90eV) using a fluorine-based RIE plasma (SF6/O2/CHF3) and the black silicon method (BSM) [1-3]. The low ion energy prevents substrate damage (electronics), mask erosion (the selectivity to metal masks is practically infinite), and makes it easy to change the profile of the trench. In the BSM the forming of "grass" or black silicon is used to find the vertical wall regime and after this the profile can be altered by changing the plasma chemistry (power, pressure, or flows) with the help of diagrams.

Characteristic for MEMS are the dimensions of structures that can range from several microns up to millimetres. In dry etching, this type of nonuniformities in dimensions (i.e. pattern density and feature size) will give rise to differences in etch rate and profiles [4]. For etching silicon, evidence is found that the nonuniformity is controlled by ion bowing; the deflection (and capture) of impinging ions to the conducting sidewall of a trench. The nonuniformity is found to be suppressed in making the trench walls more insulating [5].

In this article a comprehensive overview of the BSM will be given [3] illustrated with a case study of scanning probe microscopy [6]. Design considerations are given in which the normally used cantilever/tip configuration is replaced by an xy-stage/ tip construction [7]. To fulfil the process requirements the BSM is presented as a powerful tool to find the process conditions for the desired structures; e.g. deep trenches or needles, both with a high aspect ratio.

2. THE BLACK SILICON METHOD

An easy way to find the recipe for any RIE system for the etching of silicon giving a vertical wall profile, together with the influence of various parameters on this profile, is accomplished with the so-called black silicon method (BSM). This method uses the fact that the silicon appears black when it is etched exactly anisotropic. Before the BSM is formulated, the chemistry is treated, the reason for the blackening will be explained, and a way to deal with this effect will be described.

The SF6/O2/CHF3 chemistry: In an SF6/O2/CHF3 plasma, each gas has a known specific function and influence, so the etched profile is easily controlled just by changing the flow rate of one of these gases [1-3]. In such a plasma SF6 produces the F* radicals for the chemical etching of the silicon forming the volatile SiF4 (Figure 1), oxygen creates the O* radicals to passivate the silicon surface with SiOxFy, and CHF3 (or SF6) is the source of CFx+ (or SFx+) ions, responsible for the removal of the SiOxFy layer at the bottom of the etching trenches forming the volatile COxFy (or SOxFy).

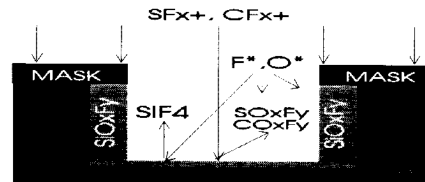

Figure 1: The SF6/O2/CHF3 chemistry.

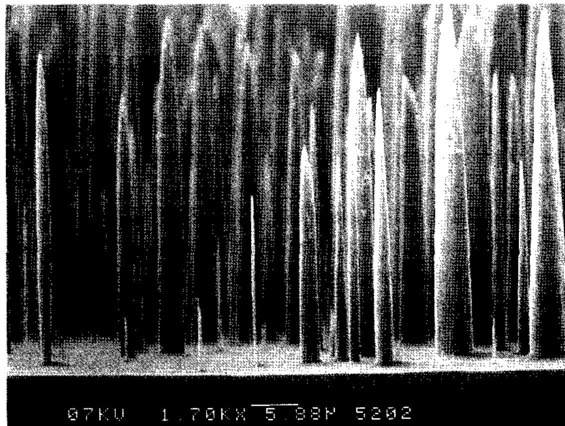

Figure 2. Black silicon surrounding etched structures.

The origin of black silicon: As stated in the above there is a constant competition between the fluorine radicals that etch and the oxygen radicals that passivate the silicon. At a certain oxygen content there is such a balance between the etching and the passivation that a nearly vertical wall results. At the same moment native oxide, dust, et cetera will act as micro masks and, because of the directional etching, spikes will appear (Figure 2). These spikes consist of a silicon body with a thin passivating siliconoxyfluoride skin. If the length of the spikes exceed the wavelength of incoming light, this light will be "caught" in the areas between the spikes and the silicon surface appears black. The origin of micro masks is caused by native oxide, dust, and so on which is already on the wafer before etching. But, they are also formed during the etching because silicon oxide particles coming from the plasma are adsorbing at the silicon surface or because of the oxidation of the silicon surface together with the angle dependent ion etching of this oxide layer. Another source of particles during etching which will act as micro masks is the resputtering of mask material due to imparting ions.

Preventing black silicon: It is possible to prevent spikes from forming by constantly etching the features with a slightly negative undercut. At the same time, this is an excellent way to control the smoothness of the substrate surface, barely limiting the feature size density. In this study the addition of CHF3 to an SF6/O2 plasma is described and its ability to prevent grass.

The formulation of the black silicon method:

1. *Coarse tuning the profile:* Place a piece of Si in the reactor and adjust the preferred power and pressure for an SF6/O2 plasma (e.g. $1W/cm^2$, 100mTorr, 100 sccm SF6- and 1sccm O2-flow). Etch ca. 1 micron of silicon, open the process chamber, and look if the silicon is black. If not, do the same again but increase the oxygen flow. Proceed with this sequence until it is black. If it stays clean, add extra Si in the reactor to increase the loading until the Si appears black. Increasing the oxygen too much, still will give rise to black-, or better grey-, silicon since there exists a positively tapered profile with hardly any underetching (Figure 3a).

2. *Cleaning the surface:* After the black silicon regime is found add CHF3 to the mixture and increase this flow until the wafer is clean again. Too much CHF3 will make the profiles isotropic (and smooth) because the CFx species are scavenging the oxygen radicals which are needed for the blocking layer.

3. *Fine tuning the profile*: Now a wafer with the mask pattern of interest is inserted in the reactor and the etched profile is checked. Add extra silicon into the reactor chamber until the exposed silicon area is the same as in step 1 and 2. Increasing the SF6 content will create a more isotropic profile. Adding more oxygen will make the profile positively tapered and extra CHF3 will make it more negatively tapered (Figure 3a). Adding at the same time O2 and CHF3 with the correct balance will create very smooth and nearly vertical walls. Increasing the pressure or decreasing the power will make the profile more positively tapered. In figure 3a/b the influence of the O2/CHF3 flow and the pressure/power on the profile is given.

As can be concluded from figure 3, vertical walls can be achieved for any pressure, power, O2-, CHF3-, or SF6-flow. This is an important conclusion because now we are able to create any d.c. self-bias we want without changing the profile. For instance, it is possible to develop very low bias voltages (<20eV) at the higher pressures giving very high mask selectivity, while maintaining the profile. In such cases the etched silicon bottom and the sidewalls are nearly perfect (Figure 4).

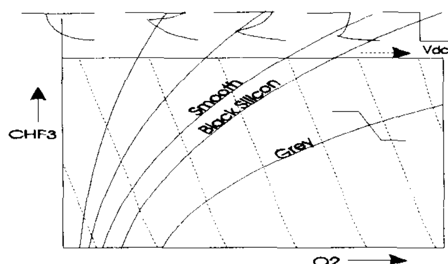

Figure 3a: The influence of the flows on the profile.

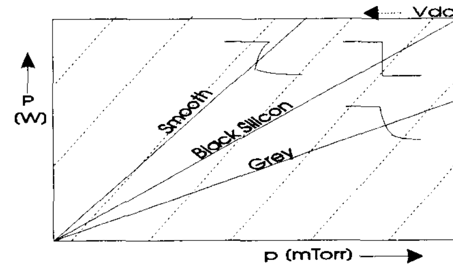

Figure 3b: The influence of the power and pressure on the profile.

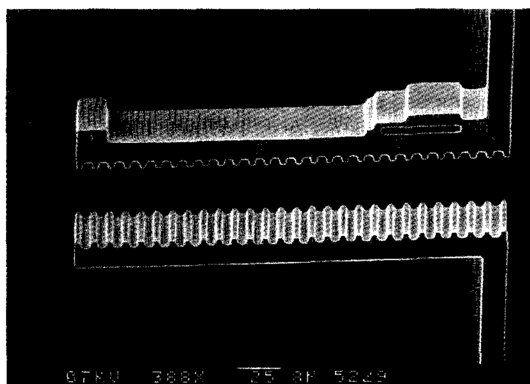

Figure 4: Smooth surfaces after etching.

3. SCANNING PROBE MICROSCOPY

In a short historical overview the developments in the field of scanning probe microscopy (SPM) will be presented. The fundamental aspects and operating principles are described.

History of SPM: In 1982 the first member of the family of *scanning probe microscopes*, the scanning tunneling microscope (STM), was invented [8,9]. In the STM a sharp conducting tip is brought in close proximity of a sample surface. Applying a potential difference between tunnel tip and surface, a current of electrons may flow between tip and sample. Scanning the tip in a raster pattern over the surface then yields a topographic image of the sample surface under investigation. The main limitation of the STM is the fact that only conducting or semiconducting samples can be imaged.

To circumvent this problem of sample conductivity, the *atomic force microscope* (AFM) or *scanning force microscope* was introduced [10]. In the AFM, a sharp tip is mounted at the free end of a cantilever. While scanning the tip over the surface, forces acting between tip and sample will deflect the cantilever. These deflections can be measured by a tunneling tip on the back of the cantilever. Conceptually, this *contact mode* (or static) AFM is like using a stylus profilometer to measure the topography of surface atoms.

Not only the cantilever deflections normal to the surface can be measured, but also the forces along the surface. The measurement of the twisting movement of the cantilever gave the AFM a chemical sensitivity on the basis of differences in friction coefficient [11]. Sometimes it is therefore referred to as *friction force microscope* or the *lateral force microscope*. With this adaptation of the contact mode AFM it became possible to image domains in thin films, which were not observed in the height images [12].

Imaging soft samples in air has been a problem for years in AFM. The lateral forces tend to disrupt the sample and no stable imaging can be obtained. In 1993 the *tapping mode* AFM in air was introduced [13,14]. The lateral forces are highly diminished in this mode and it is then possible to image soft samples without much deformation.

Instead of measuring the static cantilever deflections, as in contact AFM, in *noncontact* AFM the cantilever is oscillated near or at its resonance frequency [15]. In this mode, the long-range attractive forces, such as Van der Waals, electrostatic and magnetic, can be probed. The gradient of the force acts to modify the effective spring constant of the cantilever. By measuring the change in amplitude, phase or oscillation frequency, these forces can be detected with high sensitivity. If only the attractive Van der Waals interaction is present, the height profile of the sample can be imaged by using a feedback loop, which keeps tip-sample spacing at a constant value. The resolution in noncontact AFM is determined by the sharpness of the tip and the tip sample distance. Thus the contact mode AFM works in the *repulsive* regime of the interaction potential between tip and sample and the noncontact mode AFM in the *attractive* regime.

In addition to the attractive Van der Waals force, electrostatic forces can be detected if both the object and the tip have a net electric charge, or either tip or sample is polarisable. Ferroelectric domain walls in ferroelectric-ferroelastic materials [16] and localised charges on insulating surfaces [17] have been imaged with this *electrostatic force microscope* (EFM).

Magnetic forces between tip and object occur when there is a net magnetisation on both the tip and the object. Imaging bit patterns in magnetic [18] and magneto-optical recording media is only one of the applications of this *magnetic force microscope* (MFM). Resolution on the order of 20 nm has been obtained [19].

Scanning near-field optical microscopy (SNOM) allows the investigation of optical properties on sub-wavelength scales. The near-field optical interaction between a sharp probe-tip and a sample of interest can be exploited to image, spectroscopically probe, or modify surfaces at a resolution (down to ~12nm) inaccessible by traditional far-field techniques. Many of the attractive features of conventional optics are retained, including non-invasiveness, reliability, and low cost. In addition, most optical contrast mechanisms can be extended to the near-field regime, resulting in a technique of considerable versatility [20,21].

The number of AFM users rapidly increased after the introduction of microfabricated cantilevers in 1990 [22]. Prior to that, each AFM probe (cantilever + tip) had to be hand made one at a time. The use of a new deflection detection method, the optical beam deflection [23], in combination with these microfabricated cantile-

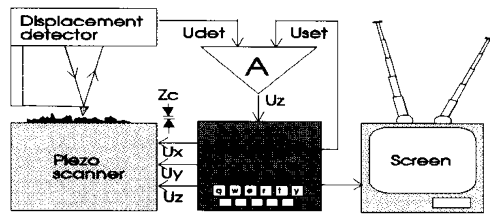

Figure 5: Schematic diagram of a standard contact AFM.

vers, greatly increased the user friendliness of the AFMs. An essential step for biological application was the demonstration that AFM can provide high-resolution images under physiological conditions (fluids) [24,25].

Fundamentals of AFM: To get a better understanding and feeling for how an AFM actually works, the essential parts will be discussed now. In figure 5 a schematic diagram of a standard contact AFM is depicted.

AFM probe: In 1990 Albrecht et al. [22] presented a microfabrication technique, making cantilevers with integrated pyramidal tips widely available. The force constants of these cantilevers range from 0.03 to 0.6 N/m and the radii of curvature of the tips are typically 30-50 nm. A sharper tip directly results in an increase of (lateral) resolution. Keller & Chou [26] showed that with the electron beam in a scanning electron microscope a small and sharp needle of carbonaceous material can be grown at the apex of the original pyramidal AFM tip. The radius of curvature can be improved to about 10 nm for these so-called supertips.

Displacement detection: The sharp tip on the cantilever is brought in contact with the sample surface. Due to the short-range repulsive interatomic forces the cantilever will be bend from its zero-position by a small amount. The most widely used displacement detector in AFM is the optical beam deflection technique. A laser beam bounces off the backside of the cantilever towards a segmented photodiode. The difference signal between the two segments is directly proportional to the displacement of the cantilever.

Scanner: The sample is scanned underneath the tip with a piezo scanner. This scanner can be a tripod arrangement of three piezo stacks or a piezo tube [27].

Data acquisition: The displacement detector yields an output voltage U_{det}, which is proportional to the normal deflection, Z_c. U_{det} is compared with the setpoint voltage U_{set} and (U_{det}-U_{set}) is amplified by an integrating amplifier. The voltage difference U_z is applied to the z electrode of the piezo tube. By this feedback loop the displacement of the cantilever Z_c, and consequently the applied force F_z (=$K_c Z_c$, where K_c is the spring constant of the cantilever), is kept at a constant value. Mapping the changes in U_z (due to height variations on the sample surface) as a function of x and y, while scanning the sample in a raster pattern, gives a topographic image of the surface.

4. DESIGN OF A SCANNING PROBE MICROSCOPE

The above mentioned standard AFM construction has some drawbacks which makes it difficult to calibrate. For example, the assemblage of probe and piezo stack together with the alignment of the laser plus photodetector makes the AFM expensive. Different types of AFM devices demand different types of tip-profiles and -radii. (Example: Contact mode AFM needs sharp tips with sharp cone-like profiles, whereas MFM needs thin cylinder-like profiles).

Problem definition: After we have found the shortcomings of previous designs of AFMs we can now define the problem: *Design an AFM device which integrates directly the probe and an xyz-stage/manipulator. The tip-profile and -radius of the probe should be controllable.*

Principle of operation: It is assumed that this phase has indicated that a comb-driven xy-stage configuration is most suitable for our application. Well-designed flexures should ensure a stable manipulation in the xy-plane. Thus the piezo stack is replaced by electrostatic combs which are operated with an integrated driving voltage source.

Design: Basic characteristics of the xy-stage such as stability, non-linear behaviour, and coupling between x- and y-plane (translation as well as rotation) have already been considered and optimised with the help of (non-)linear theory and finite element analysis (FEA) [28]. In fig.6 an optimised xy-stage is shown; axial stress which is responsible for non-linear behaviour is avoided due to a folded beam structure, the electrical connection is split to avoid deflection of the stage in the Z-plane, the beam- to comb-width ratio is optimised, the construction is such that the x- and y-direction are minimally coupled and extra beams are used to avoid the rotation of a comb and thus preventing short circuit.

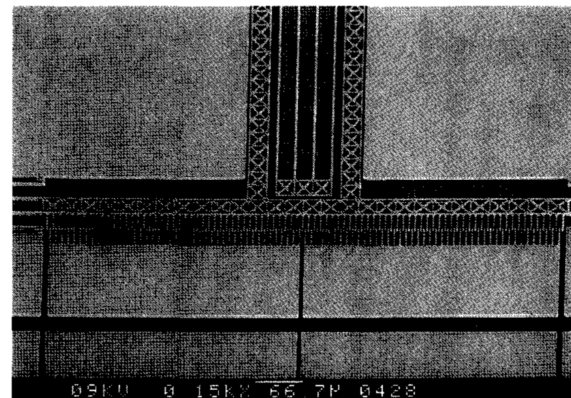

Figure 6: A comb-driven xy-stage.

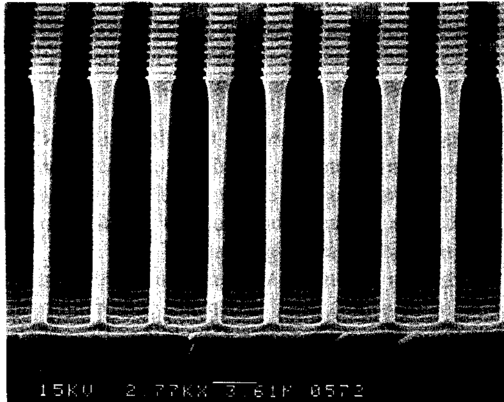

Figure 7: An array of silicon pillars for filter- or MFM applications.

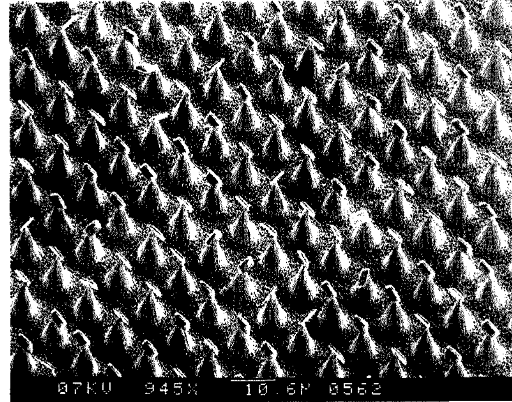

Figure 9: The same as figure 8 but just after the flip over of the mask.

A main topic in this optimisation process is the ability to create low driving voltages (<20V) which makes it possible to use this stage in fluidic environments, because electrolyses can be avoided. Many process schemes for the manufacturing of free moving stages have been under research and an overview will be presented elsewhere. Typical displacements of the MEMS are 10 microns at 50 volts and this performance is increased (25 microns at 5 volts) when operating the structures in (dielectric) liquids such as isopropanol, demiwater, or fluorinert®.

An important improvement is made possible by the integration of the translation table and the probe [7]. This is done by the use of an integrated tip on top of an xy-positioning table. The tip is integrated using standard IC technology. The integration of the electronics with the table replaces the expensive hybrid or assembling procedures normally used for standard AFM constructions. The all monocrystalline silicon xy-table has the advantage that there is *no* hysteresis or creap during the scanning of the sample making the map very reliable. Notwithstanding the importance of an highly accurate positioning table, the hart of the AFM is still the needle which should have a highly controllable (sharp) tip.

5. EXAMPLES AND CONCLUSIONS

In fig. 7-13 the high potential of the BSM is shown: All kinds of tips can be created reproducible with profiles and radii on request. In fig.7, an array of silicon needles are etched for filter applications in inkjet nozzles, biological applications such as the separation of living cells, or as probe tips for magnetic force microscopy.

Sharp positively tapered silicon tips for AFM applications can be fabricated with the BSM in allowing a controllable under etching. It is possible to fabricate spikes having an aspect ratio of 50 or more and a tip radius smaller than 5nm. To achieve such sharp tips a remarkable phenomena is used which occurs during the RIE of these tips. When an insulating mask is used for the pattern transfer, this mask will flip over after the mask is under etched. This is caused by electrostatic forces which exist during the RIE of silicon. This mask is protecting the sharp tip after that moment from incoming energetic ions, so over etching is not a big problem. In figure 8 an array of tips is shown after the RIE with still the mask (i.e. SiNx plus Al) in place. In figure 9 the

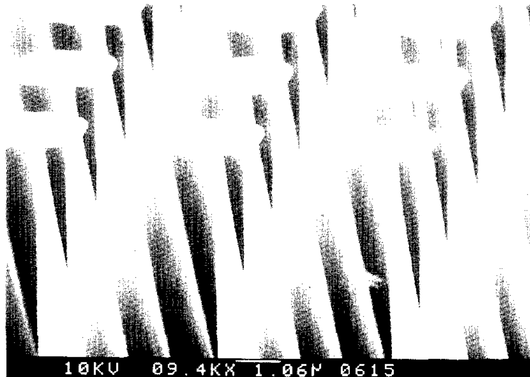

Figure 8: An array of sharp silicon needles with the mask still in place.

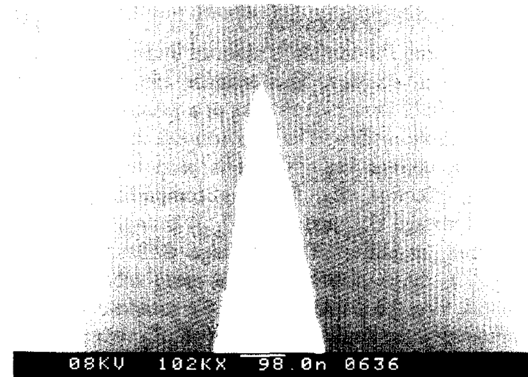

Figure 10: A 5 nm silicon tip for AFM application.

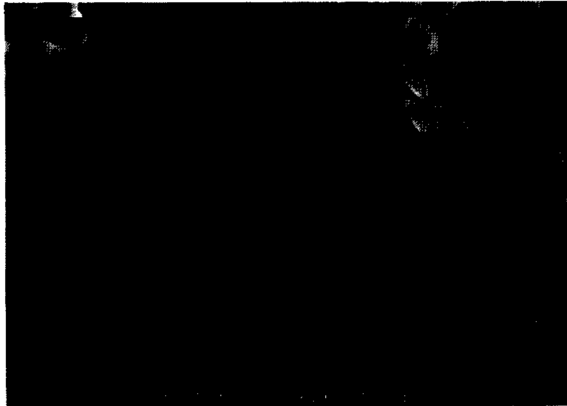

Figure 11: Needles for STM applications.

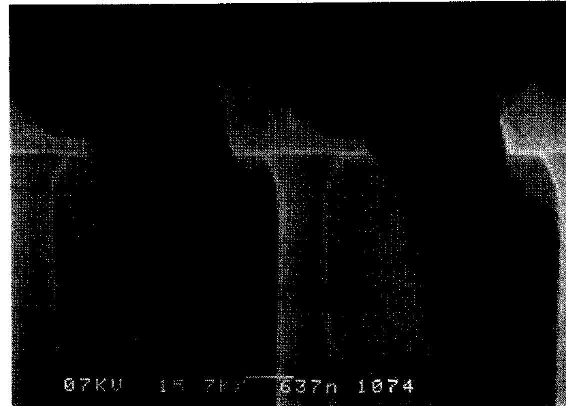

Figure 13: Close-up of figure 12.

same tips are shown after the mask-flip over and in figure 10 one tip is shown after the removal of the mask.

Changing the chemistry in a different direction (e.g. more CHF3) creates negatively tapered profiles. In figure 11 a collection of nails is shown; the heads of these nails are attached because of electrostatic forces. It is imaginable to create such tips directly *under* a fabricated cantilever. When there is also an AFM tip on top of this cantilever, it is possible to measure AFM deflection with an integrated STM tip.

In figure 12,13 typical tips for electrostatic force microscopy are shown. The tips are not sharp but are a little wider at their top. On the top of the tips, the aluminium mask is still in place (Note: The strange form of this mask is due to the lift-off process).

In conclusion, it can be stated that the BSM can be very useful in fabricating three dimensional structures for MEMS applications. Xy-tables as well as tips can be fabricated with high precision and controllable profiles. In addition, the surfaces (bottom/sidewall) are very smooth.

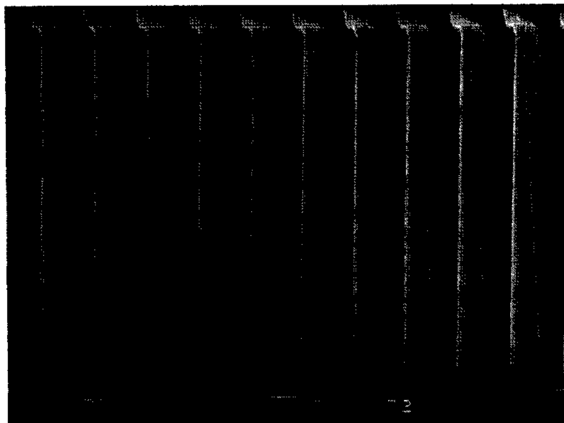

Figure 12: Spikes for EFM applications.

6. REFERENCES

[1] R.Legtenberg, H.Jansen, M.de Boer, M.Elwenspoek, *Anisotropic RIE of Si using SF6/O2/CHF3 gas mixtures*, submitted to J.Elec.Soc..

[2] H.Jansen, M.de Boer, R.Legtenberg, J.Elders, M.Elwenspoek, and J.Fluitman, EP appl.No.94202519.8.

[3] H.Jansen, M.de Boer, R.Legtenberg, and M.Elwenspoek, *The Black Silicon Method: A universal method for determining the parameter setting of a fluorine-based reactive ion etcher in deep silicon trench etching with profile control*, Proc. Micro Mechanics Europe (MME'94, Pisa, Italy), Sep. 1994.

[4] R.A.Gottscho, C.W.Jurgensen, and D.J.Vitkavage, *Microscopic uniformity in plasma etching*, J.Vac.Sci.Tech.,B.10(5), Sep.1992.

[5] H.Jansen, M.de Boer, J.Burger, R.Legtenberg, and M.Elwenspoek, *The Black Silicon method II: The effect of mask material and loading on the reactive ion etching of deep silicon trenches*, Proc. Micro and Nano Engineering (MNE, Davos, Switzerland), Sep. 1994, p.312-313.

[6] C.A.J.Putman, *Development of an atomic force microscope for biological applications*, Ph.D thesis, University of Twente, April 1994.

[7] V.J.Jaecklin, C.Linder, N.F.de Rooij, and J.-M.Moret, *Micromechanical comb actuators with low driving voltages*, J.Micromech.Microeng.2 (1992).

[8] G.Binnig, H.Rohrer, C.Gerber, and E.Weibel, Appl.Phys.Lett. 40, 178, (1982).

[9] G.Binnig, H.Rohrer, C.Gerber, and E.Weibel, Phys.Rev.Lett. 49, 57 ,'82.

[10] G.Binnig, C.F.Quate, and C.Gerber, Phys.Rev.Lett. 56, 930 (1986).

[11] Y.Martin, C.C.Williams, and H.K.Wickramasinghe, J.Appl.Phys. 61, 4723, (1987).

[12] R.M.Overney, E.Meyer, J.Frommer, D.Brodbeck, R.Lüthi, L.Howald, H.J.Günterodt, M.Fujihara, H.Takano, and Y.Gotoh, Nature 359, 133 (1992)

[13] Q.Zhong, D.Inniss, K.Kjoller, and V.Elings, Surf.Sci.Lett. 290, L688 (1993).

[14] Digital Instruments, Santa Barbara, Ca., USA.

[15] O.Marti, J.Colchero, and J.Mlynek, Nanotechnol., 1, 141, (1990).

[16] F.Saurenbach and B.D.Terris, Appl.Phys.Lett. 56, 1703 (1990).

[17] B.D.Terris, J.E.Stern, D.Rugar, and H.J.Mamin, J.Vac.Sci.Technol. A 8, 374 (1990).

[18] D.Rugar, H.J.Mamin, and P.Guenthner, Appl.Phys.Lett. 55, 2588 (1989).

[19] P.Grütter, T.Jung, H.Heinzelmann, A.Wadas, E.Meyer, H.R.Hidber, and H.-J.Günterodt, J.Appl.Phys. 67, 1437 (1990).

[20] E.Betzig and J.K.Trautman, Science, Vol. 257 (1992).

[21] H.Heinzelmann and D.W.Pohl, Appl.Phys.A, Spec. issue on Scanning Probe Microscopies (1994).

[22] T.R.Albrecht, S.Akamine, T.E.Carver, C.F.Quate, J.Vac.Sci.Technol. A 8, 3386 (1990).

[23] G.Meyer and N.Amer, Appl.Phys.Lett. 53, 2400 (1988).

[24] O.Marti, B.Drake, and P.K.Hansma, Appl.Phys.Lett. 51, 484 (1987).

[25] B.Drake, C.B.Prater, A.L.Weisenhorn, S.A.C.Gould, T.T.Albrecht, C.F.Quate, D.S.Cannell, H.G.Hansma, and P.K.Hansma, Science 243, 1586 (1989).

[26] D.Keller and C.C.Chou, Surf.Sci. 268, 333 (1992).

[27] G.Binnig and D.P.E.Smith, Rev.Sci.Instrum. 57, 1688 (1986).

[28] H.Jansen, R.Verhagen, and M.Elwenspoek, *The Black Silicon Method III: Design rules, modelling, optimisation, and performance of precision systems for scanning probe, gripping, and other MEMS applications*, Sem. on handling and assembly of microparts, November 14th, 1994, Vienna.

Best Copy Available